# Testing Pseudo-Goldstone Dark Matter

*Bohdan GRZADKOWSKI*

*University of Warsaw*

Motivations

- There exists a simple model of Abelian vector dark matter (VDM), that implies an existence of two scalar degrees of freedom, that mix through their mass matrix, resulting in $h_1$ (SM-like) and $h_2$ mass eigenstates and a mixing angle $\alpha$,

- The VDM is similar to a model of pseudo-Goldstone dark matter, in which a DM candidate is an imaginary component (odd under stabilizing symmetry) of an extra complex scalar field added to the SM. The real component (even under stabilizing symmetry) develops a vacuum expectation value and mixes with the SM Higgs doublet, so there are also two scalar degrees of freedom, $h_1$ (SM-like) and $h_2$ and a mixing angle $\alpha$.

- This project was an attempt to investigate if it is possible to distinguish the two models. In other words we were seeking measurements that could be performed in near future that could disentangle the two models.

# Testing Pseudo-Goldstone Dark Matter

*Bohdan GRZADKOWSKI*
*University of Warsaw*

- Motivations

- Pseudo-Goldstone dark matter (pGDM) model

- Vector dark matter (VDM) model

- Direct detection of the vector and the pseudo-Goldstone dark matter

- Scans over parameter space

- Dark matter at $e^+e^-$ colliders

- Summary

⬦ D. Azevedo, M. Duch, BG, D. Huang, M. Iglicki, R. Santos, "One-loop contribution to dark matter-nucleon scattering in the pseudoscalar dark matter model", JHEP 1901 (2019) 138, e-Print: arXiv:1810.06105,

⬦ D. Azevedo, M. Duch, BG, D. Huang, M. Iglicki, R. Santos, "Testing scalar versus vector dark matter", Phys.Rev. D99 (2019) no.1, 015017, arXiv:1808.01598,

⬦ M. Duch, BG, M. McGarrie, "A stable Higgs portal with vector dark matter", JHEP 1509 (2015) 162

# Pseudo-Godstone dark matter (pGDM) model

- J. Cline, T. Toma, "Pseudo-Goldstone dark matter confronts cosmic ray and collider anomalies", arXiv:1906.02175,

- D. Karamitros, "Pseudo Nambu-Goldstone Dark Matter: Examples of Vanishing Direct Detection Cross Section", Phys.Rev. D99 (2019) no.9, 095036,

- K. Kannike, M. Raidal, "Phase Transitions and Gravitational Wave Tests of Pseudo-Goldstone Dark Matter in the Softly Broken $U(1)$ Scalar Singlet Model", Phys.Rev. D99 (2019) no.11, 115010,

- T. Alanne, M. Heikinheimo, V. Keus, N. Koivunen, K. Tuominen, "Direct and indirect probes of Goldstone dark matter", Phys.Rev. D99 (2019) no.7, 075028,

- K Huitu, N. Koivunen, O. Lebedev, S. Mondal, T. Toma, "Probing pseudo-Goldstone dark matter at the LHC", arXiv:1812.05952,

- K. Ghorbani, P. Hossein Ghorbani, "Leading Loop Effects in Pseudoscalar-Higgs Portal Dark Matter", JHEP 1905 (2019) 096,

- K. Ishiwata, T. Toma, "Probing pseudo Nambu-Goldstone boson dark matter at loop level", JHEP 1812 (2018) 089,

- D. Azevedo, M. Duch, BG, D. Huang, M. Iglicki, R. Santos, "One-loop contribution to dark matter-nucleon scattering in the pseudoscalar dark matter model", JHEP 1901 (2019) 138,

- D. Azevedo, M. Duch, BG, D. Huang, M. Iglicki, R. Santos, "Testing scalar versus vector dark matter", Phys.Rev. D99 (2019) no.1, 015017,

- C. Gross, O. Lebedev, and T. Toma, "Cancellation Mechanism for Dark-Matter–Nucleon Interaction", Phys. Rev. Lett. 119 (2017), no. 19 191801.

$$S = \frac{1}{\sqrt{2}}(v_S + \phi_S + iA) \quad , \quad H^0 = \frac{1}{\sqrt{2}}(v + \phi_H + i\sigma_H) \text{ where } H = \begin{pmatrix} H^+ \\ H^0 \end{pmatrix}.$$

$$V = -\mu_H^2|H|^2 + \lambda_H|H|^4 - \mu_S^2|S|^2 + \lambda_S|S|^4 + \kappa|S|^2|H|^2 + (\mu^2 S^2 + \text{H.c.})$$

<u>Positivity</u>: $\lambda_H > 0, \quad \lambda_S > 0, \quad \kappa > -2\sqrt{\lambda_H \lambda_S}$

<u>Symmetries</u>:

- $\mu^2 \neq 0$ breaks $U(1)$ softly to residual $Z_2 : S \to -S$,

- rephase $S$ such that $\text{Im}\,\mu^2 = 0$ (basis choice),

- $V \ni \mu^2(S^2 + S^{*\,2})$, then symmetry $S \xrightarrow{C} S^*$ ($\phi_S \to \phi_S$ and $A \to -A$) reveals itself,

- global minimum at $\langle S \rangle = \frac{v_S}{\sqrt{2}}$ with $v_S$ being real, so $C$ is unbroken and $A$ is a stable DM candidate, $m_A^2 \propto \mu^2$, if $\mu^2 \to 0$ then $A$ becomes a Goldstone boson of broken $U(1)$,

$$S = \frac{1}{\sqrt{2}}(v_S + \phi_S + iA) \quad , \quad H^0 = \frac{1}{\sqrt{2}}(v + \phi_H + i\sigma_H) \ \text{ where } \ H = \begin{pmatrix} H^+ \\ H^0 \end{pmatrix}.$$

$$\mathcal{M}^2 = \begin{pmatrix} 2\lambda_H v^2 & \kappa v v_S & 0 \\ \kappa v v_S & 2\lambda_S v_S^2 & 0 \\ 0 & 0 & -4\mu^2 \end{pmatrix}$$

$$\mathcal{M}^2_{\text{diag}} = \begin{pmatrix} m_1^2 & 0 \\ 0 & m_2^2 \end{pmatrix}, \quad R = \begin{pmatrix} \cos\alpha & -\sin\alpha \\ \sin\alpha & \cos\alpha \end{pmatrix}, \quad \begin{pmatrix} h_1 \\ h_2 \end{pmatrix} = R^{-1} \begin{pmatrix} \phi_H \\ \phi_S \end{pmatrix},$$

$$A^2 h_i \ = \ ?$$

$$V \ni \lambda_S |S|^4 + \kappa |S|^2 |H|^2 \ni \frac{A^2}{2}(2\lambda_S v_S \phi_S + \kappa v \phi_H) = \frac{A^2}{2v_S}(\sin\alpha \, m_1^2 h_1 + \cos\alpha \, m_2^2 h_2)$$

## The Vector Dark Matter (VDM) model

- T. Hambye, "Hidden vector dark matter", JHEP 0901 (2009) 028,

- O. Lebedev, H. M. Lee, and Y. Mambrini, "Vector Higgs-portal dark matter and the invisible Higgs", Phys.Lett. B707 (2012) 570,

- Y. Farzan and A. R. Akbarieh, "VDM: A model for Vector Dark Matter", JCAP 1210 (2012) 026,

- S. Baek, P. Ko, W.-I. Park, and E. Senaha, "Higgs Portal Vector Dark Matter : Revisited", JHEP 1305 (2013) 036,

- Ch. Gross, O. Lebedev, Y. Mambrini, "Non-Abelian gauge fields as dark matter", arXiv:1505.07480,

- . . .

The model:

- extra $U(1)_X$ gauge symmetry $(A_X^\mu)$, <span style="color:red">DM candidate: $A_X^\mu$,</span>

- a complex scalar field $S$, whose vev generates a mass for the $U(1)$'s vector field, $S = (0, \mathbf{1}, \mathbf{1}, 1)$ under $U(1)_Y \times SU(2)_L \times SU(3)_c \times U(1)_X$.

- SM fields neutral under $U(1)_X$,

- in order to ensure stability of the new vector boson a $\mathbb{Z}_2$ symmetry is assumed to forbid $U(1)$-kinetic mixing between $U(1)_X$ and $U(1)_Y$. The extra gauge boson $A_\mu$ and the scalar $S$ transform under $\mathbb{Z}_2$ (dark charge conjugation) as follows

$$A_X^\mu \xrightarrow{C} -A_X^\mu \ , \ S \xrightarrow{C} S^*$$

The scalar potential

$$V = -\mu_H^2 |H|^2 + \lambda_H |H|^4 - \mu_S^2 |S|^2 + \lambda_S |S|^4 + \kappa |S|^2 |H|^2.$$

The vector bosons masses:

$$m_W = \frac{1}{2}gv, \quad m_Z = \frac{1}{2}\sqrt{g^2 + g'^2}\,v \quad \text{and} \quad m_X = g_X v_S,$$

where

$$\langle H \rangle = \begin{pmatrix} 0 \\ \frac{v}{\sqrt{2}} \end{pmatrix} \quad \text{and} \quad \langle S \rangle = \frac{v_S}{\sqrt{2}}$$

Positivity of the potential implies

$$\lambda_H > 0, \quad \lambda_S > 0, \quad \kappa > -2\sqrt{\lambda_H \lambda_S}.$$

The minimization conditions for scalar fields

$$(2\lambda_H v^2 + \kappa v_S^2 - 2\mu_H^2)v = 0 \quad \text{and} \quad (\kappa v^2 + 2\lambda_S v_S^2 - 2\mu_S^2)v_S = 0$$

For $\kappa^2 < 4\lambda_H\lambda_S$ the global minimum is

$$v^2 = \frac{4\lambda_S\mu_H^2 - 2\kappa\mu_S^2}{4\lambda_H\lambda_S - \kappa^2} \quad \text{and} \quad v_S^2 = \frac{4\lambda_H\mu_S^2 - 2\kappa\mu_H^2}{4\lambda_H\lambda_S - \kappa^2}$$

Both scalar fields can be expanded around corresponding vev's as follows

$$S = \frac{1}{\sqrt{2}}(v_S + \phi_S + i\sigma_S) \;\;, \;\; H^0 = \frac{1}{\sqrt{2}}(v + \phi_H + i\sigma_H) \;\; \text{where} \;\; H = \begin{pmatrix} H^+ \\ H^0 \end{pmatrix}.$$

The mass squared matrix $\mathcal{M}^2$ for the fluctuations $(\phi_H, \phi_S)$ and their eigenvalues read

$$\mathcal{M}^2 = \begin{pmatrix} 2\lambda_H v^2 & \kappa v v_S \\ \kappa v v_S & 2\lambda_S v_S^2 \end{pmatrix}$$
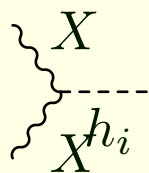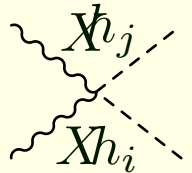
$$m_\pm^2 = \lambda_H v^2 + \lambda_S v_S^2 \pm \sqrt{\lambda_S^2 v_S^4 - 2\lambda_H\lambda_S v^2 v_S^2 + \lambda_H^2 v^4 + \kappa^2 v^2 v_S^4}$$

$$\mathcal{M}^2_{\text{diag}} = \begin{pmatrix} m_1^2 & 0 \\ 0 & m_2^2 \end{pmatrix}, \quad R = \begin{pmatrix} \cos\alpha & -\sin\alpha \\ \sin\alpha & \cos\alpha \end{pmatrix}, \quad \begin{pmatrix} h_1 \\ h_2 \end{pmatrix} = R^{-1} \begin{pmatrix} \phi_H \\ \phi_S \end{pmatrix},$$

Direct detection of the vector dark matter
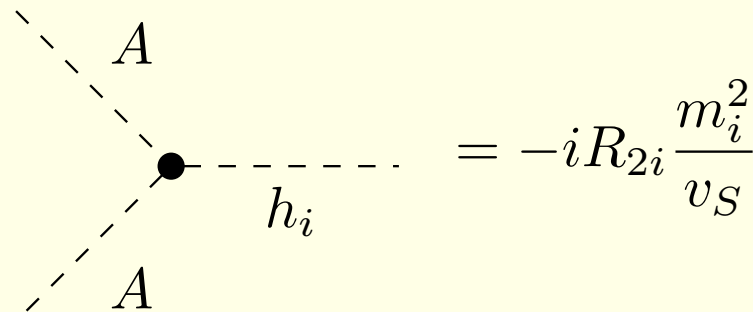
$$\mathcal{L} \ni (D_\mu S)^* D^\mu S$$

$$\Downarrow$$

| $i2m_X g_X R_{2,i}$ | $i2g_X^2 R_{2,i} R_{2,j}$ |
|---|---|
|  |  |

$$\sigma_{XN} \approx \frac{\sin^2 2\alpha}{4\pi} \frac{(m_1^2 - m_2^2)^2}{m_1^4 m_2^4} \frac{f_N^2 \mu_{XN}^2 m_X^2 m_N^2}{v^2 v_S^2}$$

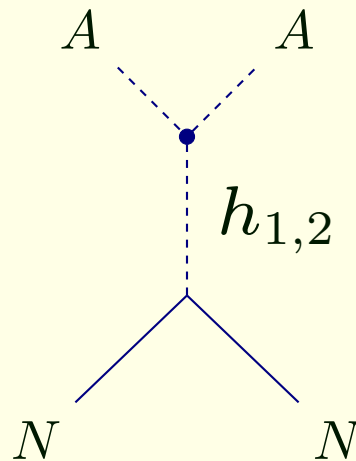where $\mu_{XN} \equiv m_X m_N / (m_X + m_N)$

$$V \supset \frac{A^2}{2}(2\lambda_S v_S \phi_S + \kappa v \phi_H) = \frac{A^2}{2v_S}(\sin\alpha\, m_1^2 h_1 + \cos\alpha\, m_2^2 h_2)\,,$$



$$= -iR_{2i}\frac{m_i^2}{v_S}$$

The corresponding amplitude for the spin-independent DM nuclear recoils reads:

The DM direct detection signals are naturally suppressed in the pGDM model.

$$V \supset \frac{A^2}{2}(2\lambda_S v_S \phi_S + \kappa v \phi_H) = \frac{A^2}{2v_S}(\sin\alpha\, m_1^2 h_1 + \cos\alpha\, m_2^2 h_2)\,,$$



$$= -iR_{2i}\frac{m_i^2}{v_S}$$

The corresponding amplitude for the spin-independent DM nuclear recoils reads:

$$
\begin{aligned}
i\mathcal{M} &= -i\frac{\sin 2\alpha\, f_N m_N}{2vv_S}\left(\frac{m_1^2}{q^2-m_1^2} - \frac{m_2^2}{q^2-m_2^2}\right)\bar{u}_N(p_4)u_N(p_2) \\
&\approx -i\frac{\sin 2\alpha\, f_N m_N}{2vv_S}\left(\frac{m_1^2 - m_2^2}{m_1^2 m_2^2}\right)q^2 \bar{u}_N(p_4)u_N(p_2)\,.
\end{aligned}
$$

$$S = \frac{1}{\sqrt{2}}(v_s + \phi_S)e^{iA/v_s} \, ,$$

- $A$ is odd under the $Z_2$ symmetry transformation $S \leftrightarrow S^*$, it is DM candidate.

- The only terms that contain $A$ are the kinetic and the $U(1)$ symmetry softly-breaking terms:

$$
\begin{aligned}
\mathcal{L}_A &= \partial^\mu S^* \partial_\mu S - \frac{M^3}{\sqrt{2}}(S + S^*) - \mu^2(S^2 + S^{*2}) \\
&\supset \frac{1}{2}\partial^\mu A \partial_\mu A + \frac{1}{2}\left(4\mu^2 + \frac{M^3}{v_s}\right)A^2 + \frac{\phi_S}{v_s}\partial^\mu A \partial_\mu A + \left(4\mu^2 + \frac{M^3}{2v_s}\right)\frac{\phi_S}{v_s}A^2 \, ,
\end{aligned}
$$

so $m_A^2 = -4\mu^2 - M^3/v_s$.

- Repeatedly integrating by parts and adopting free equations of motion for $A$ and $h_i$, one finds the pseudo-Goldstone-Higgs vertices as follows

$$\mathcal{L}_A \supset \frac{1}{2}(\partial^\mu A \partial_\mu A - m_A^2 A^2) - \frac{R_{2i}}{2v_s}\left(m_i^2 + \frac{M^3}{v_S}\right)h_i A^2$$
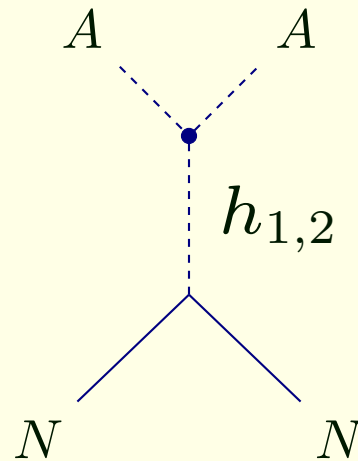
The total cross section $\sigma_{AN}$:

$$\sigma_{AN}^{(\text{tree})} \approx \frac{\sin^2 2\alpha \, f_N^2}{3\pi} \frac{m_N^2 \, \mu_{AN}^6}{m_A^2 \, v^2 v_S^2} \frac{(m_1^2 - m_2^2)^2}{m_1^4 m_2^4} v_A^4 \, ,$$

where $v_A$ is the $A$ velocity in the lab frame. Since $v_A \sim 200$ km/s, the total DM nuclear recoil cross section $\sigma_{AN}$ is greatly suppressed by the factor $v_A^4 \sim 10^{-13}$:

$$\sigma_{AN}^{(\text{tree})} \sim 10^{-70} \text{ cm}^2 \ll \sigma_{AN}^{(\text{XENON1T})} \sim 10^{-46} \text{ cm}^2$$

$$\Downarrow$$

1-loop effects are leading

- if $q^2 \to 0$ then loop corrections are expected to be UV finite,

- if $m_A^2 \propto \mu^2 \to 0$ then loop corrections should vanish.
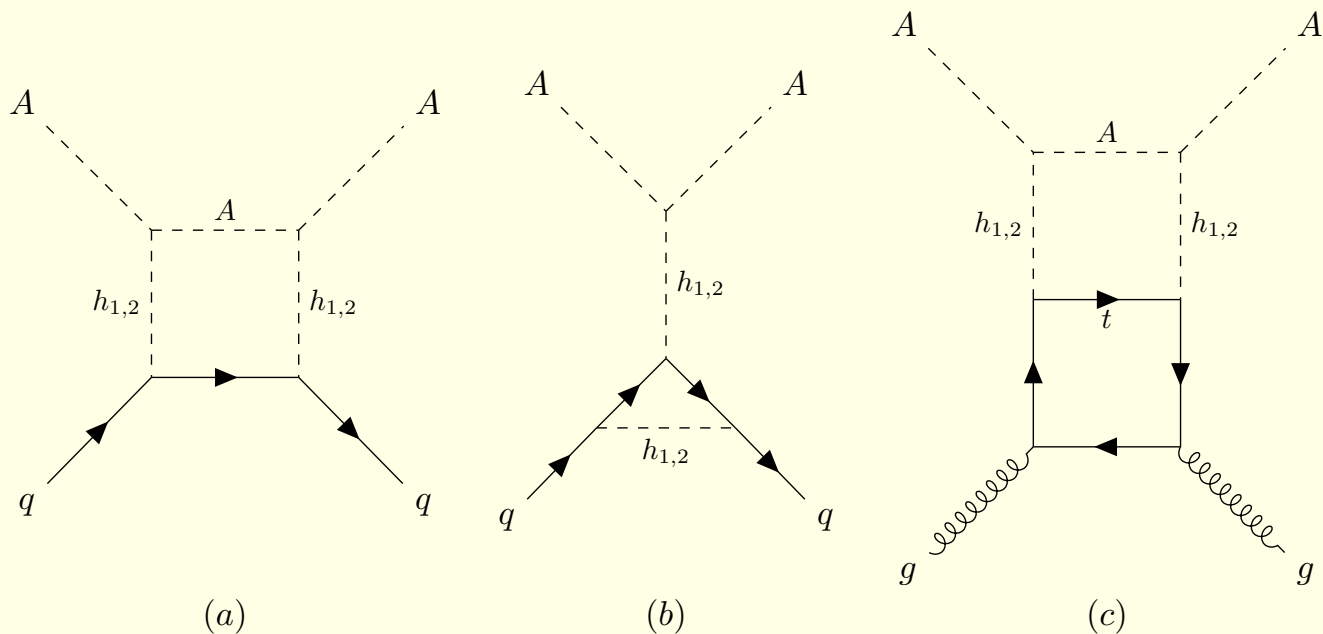
Figure 1: Examples of diagrams contributing to DM-nucleon scattering, which are discarded in our computation. Diagrams (a) and (b) represent the one-loop box and light-quark-h1;2 vertex corrected diagrams which are ignored due to the multiple Yukawa coupling suppression, while the diagram (c) is an example of DM-gluon scattering with two Higgs lines inserted into the top-quark loop, which is assumed to be subdominant.
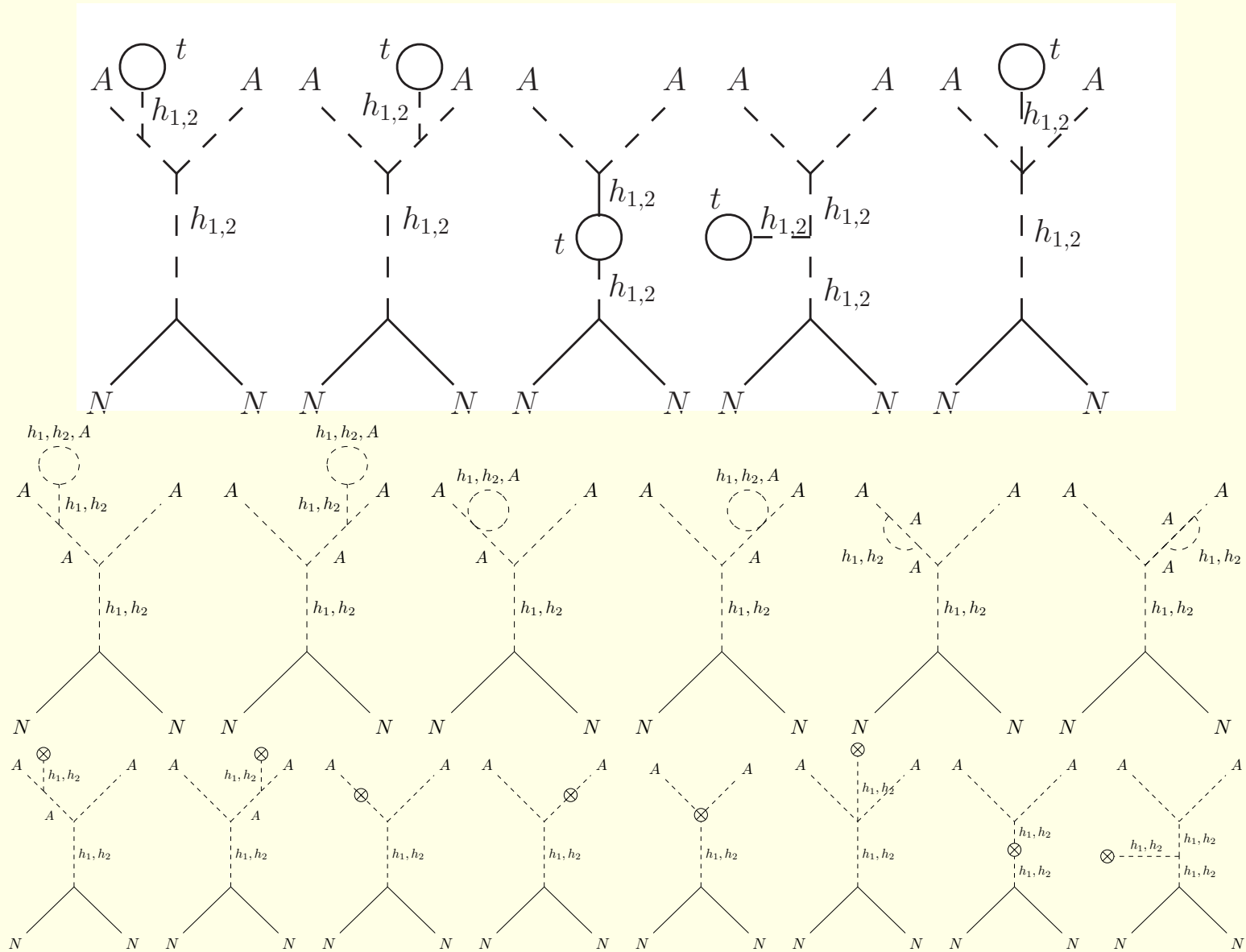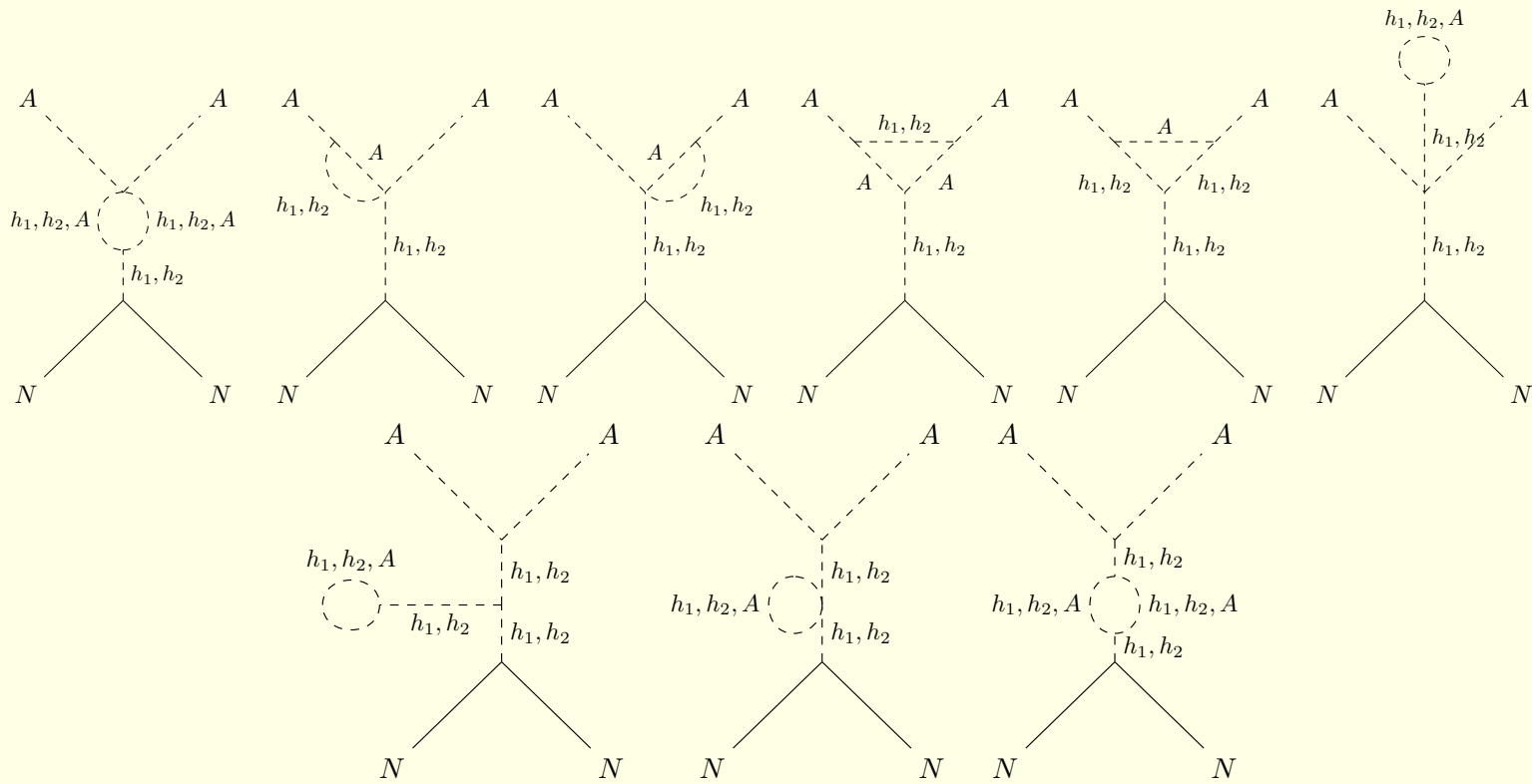
Figure 2: 1-loop diagrams that do not contribute to $A$-nucleon scattering.

Figure 3: 1-loop diagrams contributing to $A$-nucleon scattering.

$$\sigma_{AN}^{(1)} = \frac{f_N^2}{\pi v_H^2} \frac{m_N^2 \mu_{AN}^2}{m_A^2} \mathcal{F}^2 \,,$$
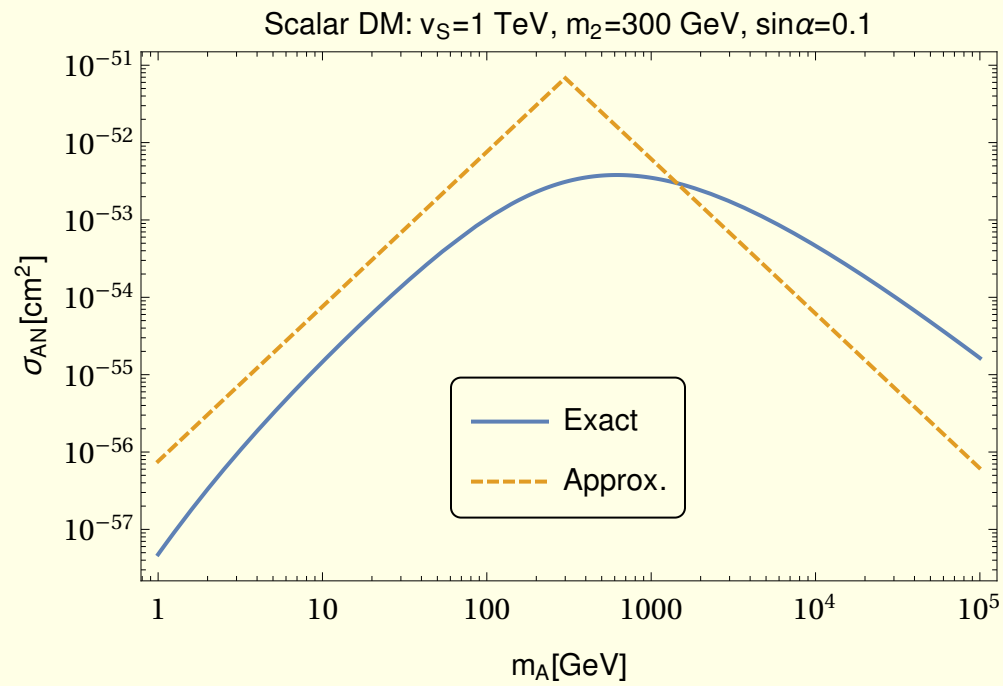
where the one-loop function $\mathcal{F}$ is defined as

$$\mathcal{F} = \frac{V_{AA1}^{(1)} c_\alpha}{m_1^2} - \frac{V_{AA2}^{(1)} s_\alpha}{m_2^2}$$

with $V_{AA1,AA2}^{(1)}$ as one-loop corrections to the vertices $h_1 A^2$ and $h_2 A^2$.

$$\begin{aligned}
\mathcal{F} &= -\frac{s_{2\alpha}(m_1^2 - m_2^2)m_A^2}{128\pi^2 v_H v_S^3 m_1^2 m_2^2} [\mathcal{A}_1 C_2(0, m_A^2, m_A^2, m_1^2, m_2^2, m_A^2) \\
&\quad + \mathcal{A}_2 D_3(0, 0, m_A^2, m_A^2, 0, m_A^2, m_1^2, m_1^2, m_2^2, m_A^2) \\
&\quad + \mathcal{A}_3 D_3(0, 0, m_A^2, m_A^2, 0, m_A^2, m_1^2, m_2^2, m_2^2, m_A^2)] \,,
\end{aligned}$$

Comments:

- The one loop amplitude $\mathcal{F}$ is UV finite in the limit of zero momentum transfer $q^2 \to 0$,

- $\mathcal{F} \to 0$ for $m_A \to 0$.

Scalar DM: $v_S$=1 TeV, $m_2$=300 GeV, $\sin\alpha$=0.1

Scalar DM: $v_S$=1 TeV, $m_A$=100 GeV, $\sin\alpha$=0.1
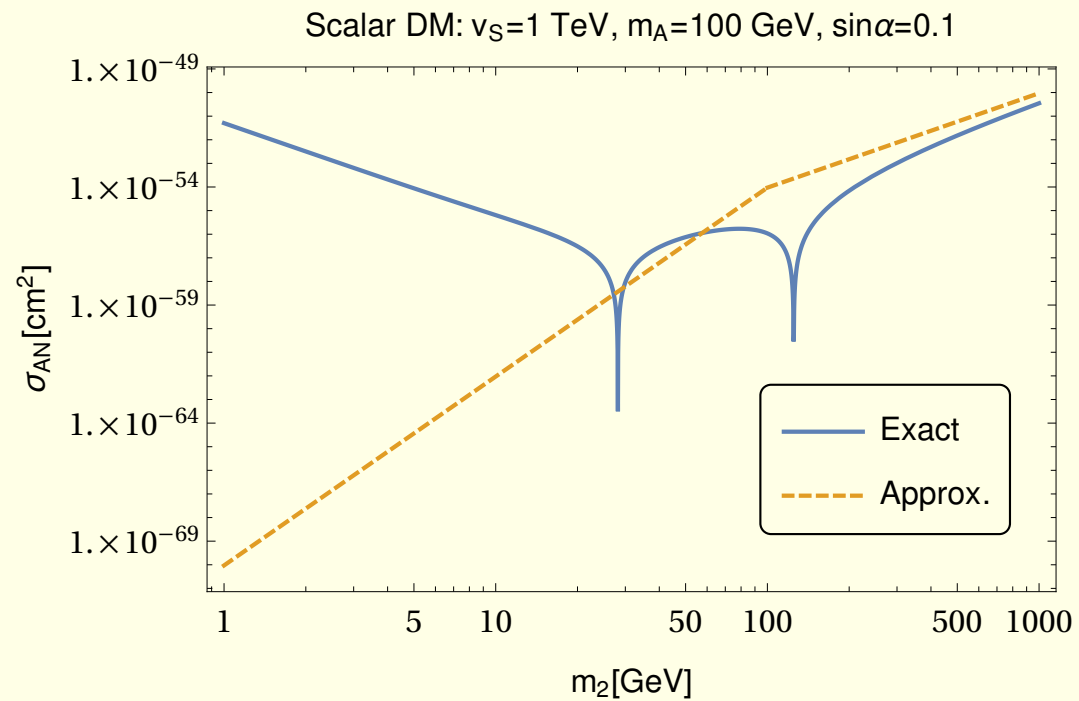
Independent parameters: $v_S, \sin\alpha, m_2$ and $m_{DM}$ ($m_A$ or $m_X$).

| Parameter | Range |
|---|---|
| Second Higgs - $m_2$ | [1,1000] GeV |
| Dark Matter - $m_{\text{DM}}$ | [1,1000] GeV |
| Singlet VEV - $v_s$ | [1,$10^7$] GeV |
| Mixing angle - $\alpha$ | $[-\frac{\pi}{4},\frac{\pi}{4}]$ |

Table 1: Scan regions for independent parameter's for both models.

We are searching for regions of the parameter space
that are only populated by one model.

Collider and/or theoretical constraints:

- The points are generated by the code ScannerS [R. Coimbra, M. O. P. Sampaio, and R. Santos, "ScannerS: Constraining the phase diagram of a complex scalar singlet at the LHC", Eur. Phys. J. C73 (2013) 2428]:

  – the potential has to be bounded from below,
  – the vacuum is chosen so that the minimum is the global one,
  – perturbative unitarity holds.

- The bound on the LHC signal strength $\mu$ for the SM Higgs is used to limit $\cos\alpha$,

- $BR(h_1 \to \mathrm{inv}) < 24\%$,

- $S$, $T$ and $U$,

- The collider bounds from LEP, Tevatron and the LHC are imposed via HiggsBounds [P. Bechtle, O. Brein, S. Heinemeyer, G. Weiglein, and K. E. Williams, "HiggsBounds: Confronting Arbitrary Higgs Sectors with Exclusion Bounds from LEP and the Tevatron",Comput. Phys. Commun. 181 (2010) 138].

Cosmological constraints:

- DM abundance: $(\Omega h^2)_{\text{DM}}^{\text{obs}} = 0.1186 \pm 0.002$ from Planck Collaboration, here we require that $(\Omega h^2)_{A,X} < 0.1186$ or we adopt $5\sigma$ allowed region,

- Direct detection: we apply the latest XENON1T upper bounds for the DM mass greater than $6$ GeV, while for lighter DM particles, the combined limits from CRESST-II and CDMSlite are utilized for $\sigma_{AN,XN}^{\text{eff}} \equiv f_{A,X}\sigma_{AN,XN}$, with

$$f_{A,X} = \frac{(\Omega h^2)_{A,X}}{(\Omega h^2)_{\text{DM}}^{\text{obs}}},$$

where $(\Omega h^2)_{A,X}$ is the calculated DM relic abundance for the pGDM $(A)$ or the VDM $(X)$.

- Indirect detection: for the DM mass range of interest, the Fermi-LAT upper bound on the DM annihilations from dwarfs is the most stringent. We use the Fermi-LAT bound on $b\bar{b}$ when $m_{A,X} \geqslant m_b$, and that on light quarks for $m_{A,X} < m_b$.
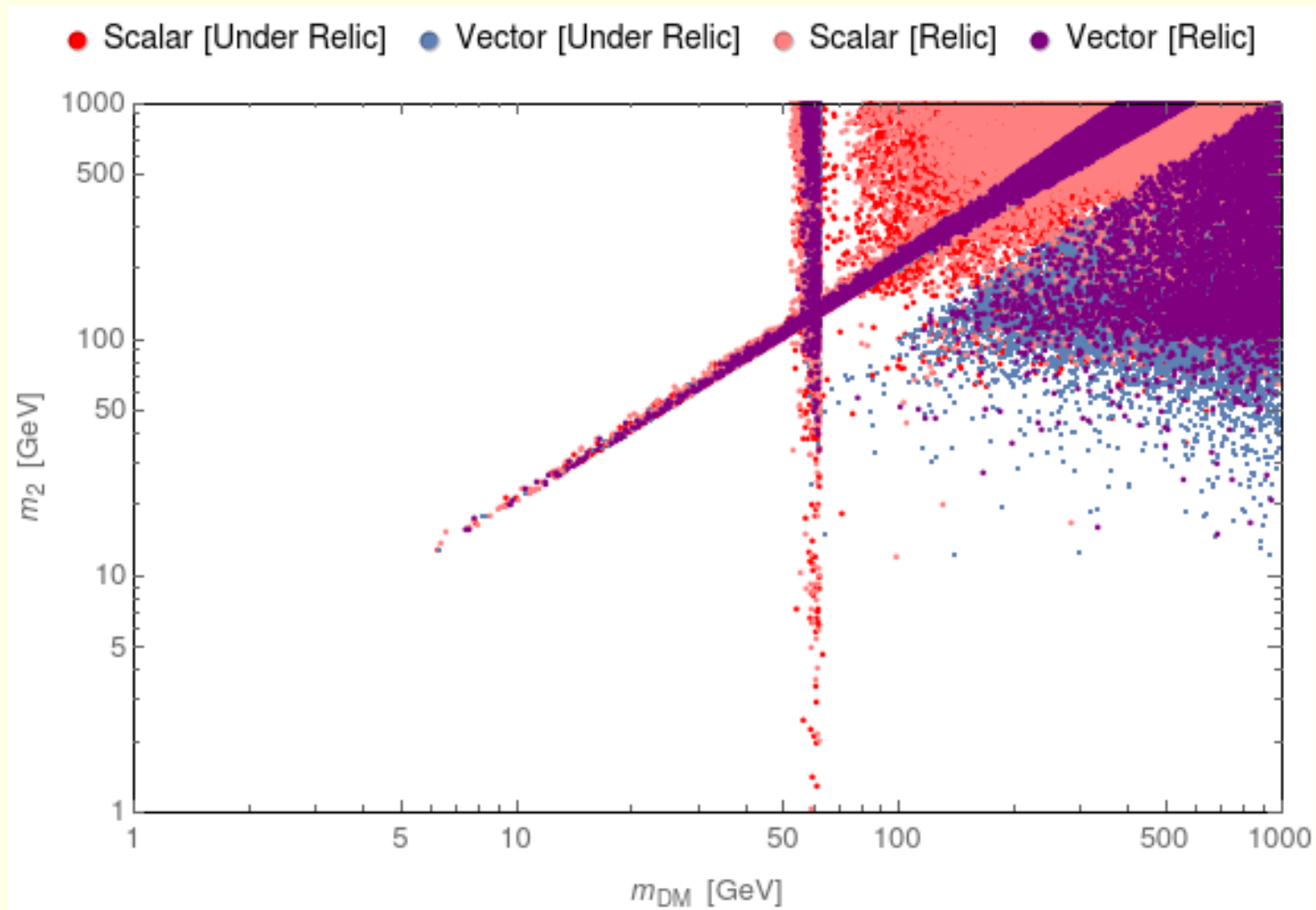
Figure 4: $m_2$ versus $m_{DM}$.

Where the models coexist:
- $m_2 \simeq 2m_{DM}$ (DM annihilation through the non-SM-like resonance $h_2$),
- $m_{DM} \simeq m_1/2$ (DM annihilation through the SM-like resonance $h_1$),

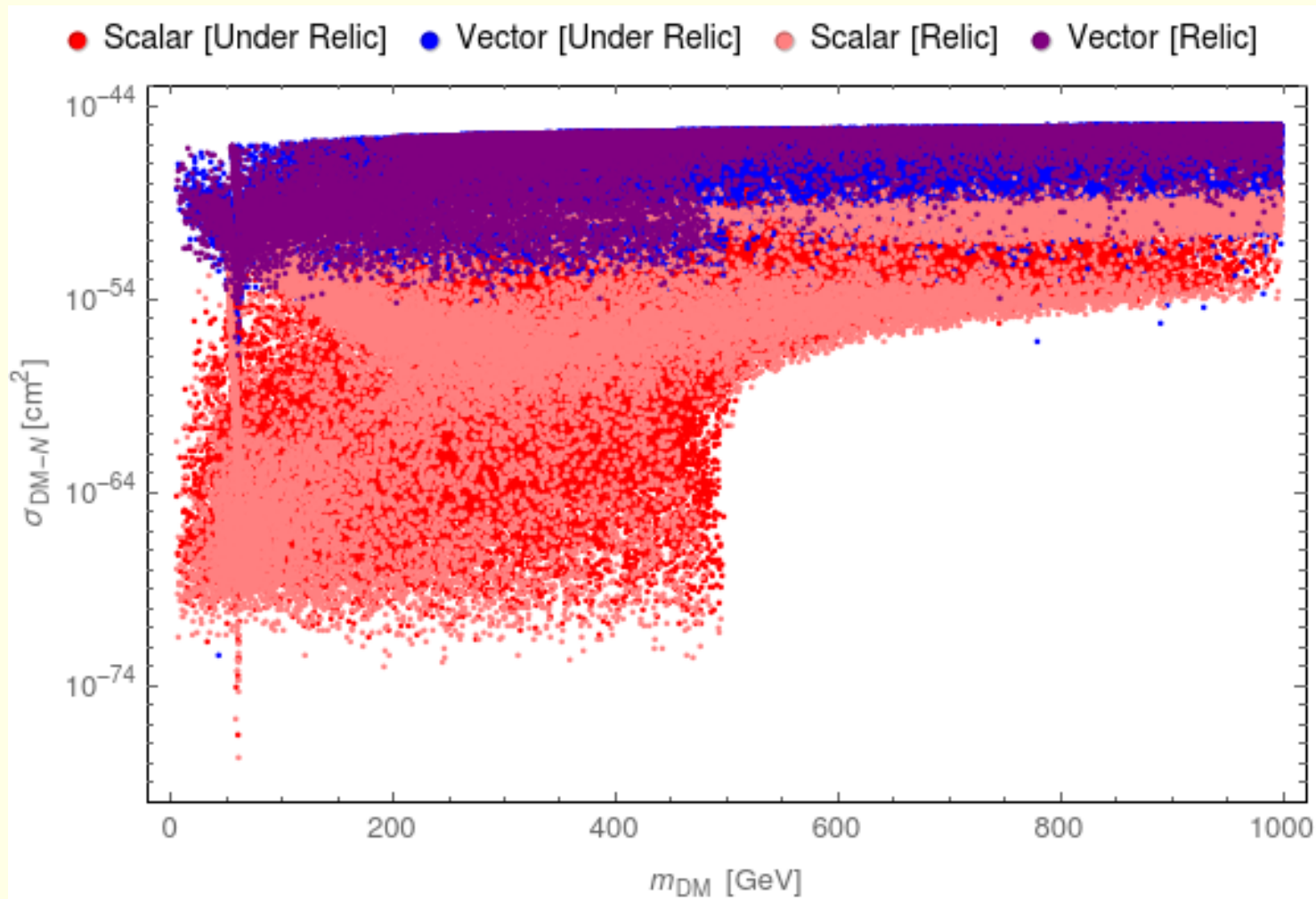pGDM and VDM could be disentangled by a measurement of $m_{DM}$ and $m_2$.

Figure 5: DM-nucleon cross-section as a function of the DM mass. Scalar DM-nucleon nucleon cross-section is computed at one-loop level. The latest results from Xenon1T are shown as the solid line that makes the upper edge of the plot.

- Suppression of $\sigma_{DM-N}$ for the pGDM model,
- $h_1$ and $h_2$ resonance effects for both the pGDM and the VDM models, $m_1 \simeq 2m_{DM}$ and $m_2 \simeq 2m_{DM}$, respectively.
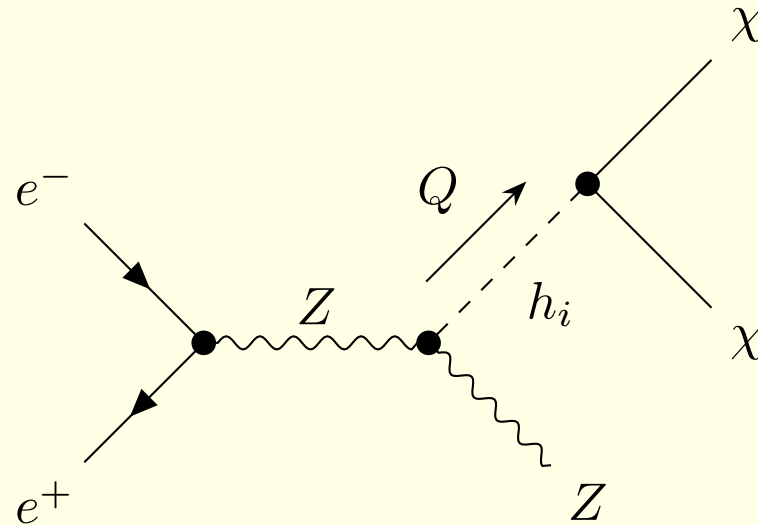
Figure 6: Feynman diagram for $e^+e^- \to Z\chi\bar{\chi}$, $\chi$ denotes the dark particle ($\chi = A, X$).

- P. Ko, H. Yokoya, "Search for Higgs portal DM at the ILC", JHEP 1608 (2016) 109,

- T. Kamon, P. Ko, J. Li "Characterizing Higgs portal dark matter models at the ILC", Eur.Phys.J. C77 (2017) no.9, 652
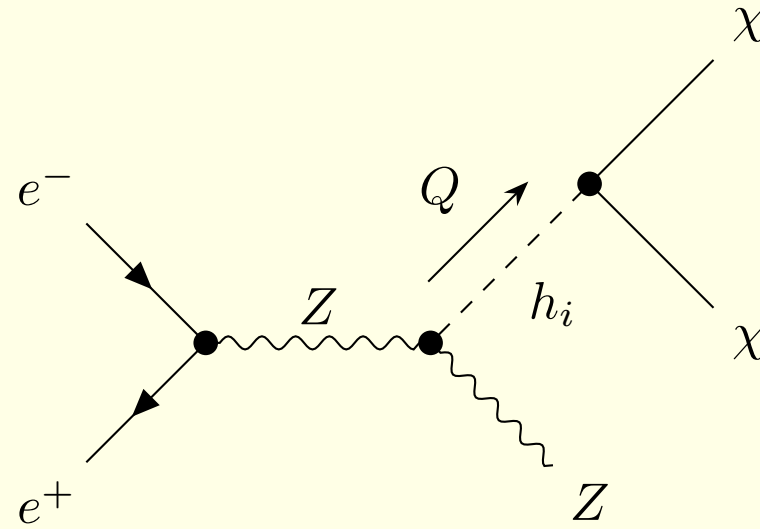
Figure 7: Feynman diagram for $e^+e^- \to Z\chi\bar{\chi}$, $\chi$ denotes the dark particle ($\chi = A, X$).

$$\frac{d\sigma}{dE_Z}(E_Z) = f(s, E_Z) \cdot \frac{\left(\frac{\sin 2\alpha}{v_S}\right)^2 \cdot \sqrt{1 - 4\frac{m_{DM}^2}{Q^2}} \cdot (m_1^2 - m_2^2)^2 \cdot Q^4}{[(Q^2 - m_1^2)^2 + (m_1\Gamma_1)^2][(Q^2 - m_2^2)^2 + (m_2\Gamma_2)^2]} \times$$

$$\times \begin{cases} 1 & \text{(pGDM)} \\ 1 - 4\frac{m_X^2}{Q^2} + 12\left(\frac{m_X^2}{Q^2}\right)^2 & \text{(VDM)} \end{cases},$$

$$\frac{2}{3} \leq 1 - 4\frac{m_X^2}{Q^2} + 12\left(\frac{m_X^2}{Q^2}\right)^2 \leq 1$$

$$Q^2 = s - 2E_Z\sqrt{s} + m_Z^2$$

$$f(s, E_Z) \equiv \frac{(1 - P_+P_-)(g_v^2 + g_a^2) + 2g_vg_a(P_+ - P_-)}{12 \cdot (2\pi)^3} \sqrt{E_Z^2 - m_Z^2} \left(2m_Z^2 + E_Z^2\right)$$

$$\times \left(\frac{g^2}{\cos\theta_W^2} \frac{1}{s - m_Z^2}\right)^2 \tag{1}$$

$$Q^2 = Q^2(s, E_Z) \equiv s - 2E_Z\sqrt{s} + m_Z^2$$

$$E_Z(Q^2 = m_i^2) = E_i \equiv \frac{s - m_i^2 + m_Z^2}{2\sqrt{s}}.$$

$$E_{\max} = \frac{s - 4m_{DM}^2 + m_Z^2}{2\sqrt{s}},$$

$$\sqrt{s} = 1.5 \text{ TeV}, \quad m_2 = 700 \text{ GeV}, \quad v_S = 5.54 \text{ TeV}$$

— two–pole case: $m_{\text{DM}} = 60$ GeV, $\sin\alpha = 0.01$
— one–pole case: $m_{\text{DM}} = 200$ GeV, $\sin\alpha = 0.05$
— no–pole case: $m_{\text{DM}} = 500$ GeV, $\sin\alpha = 0.3$
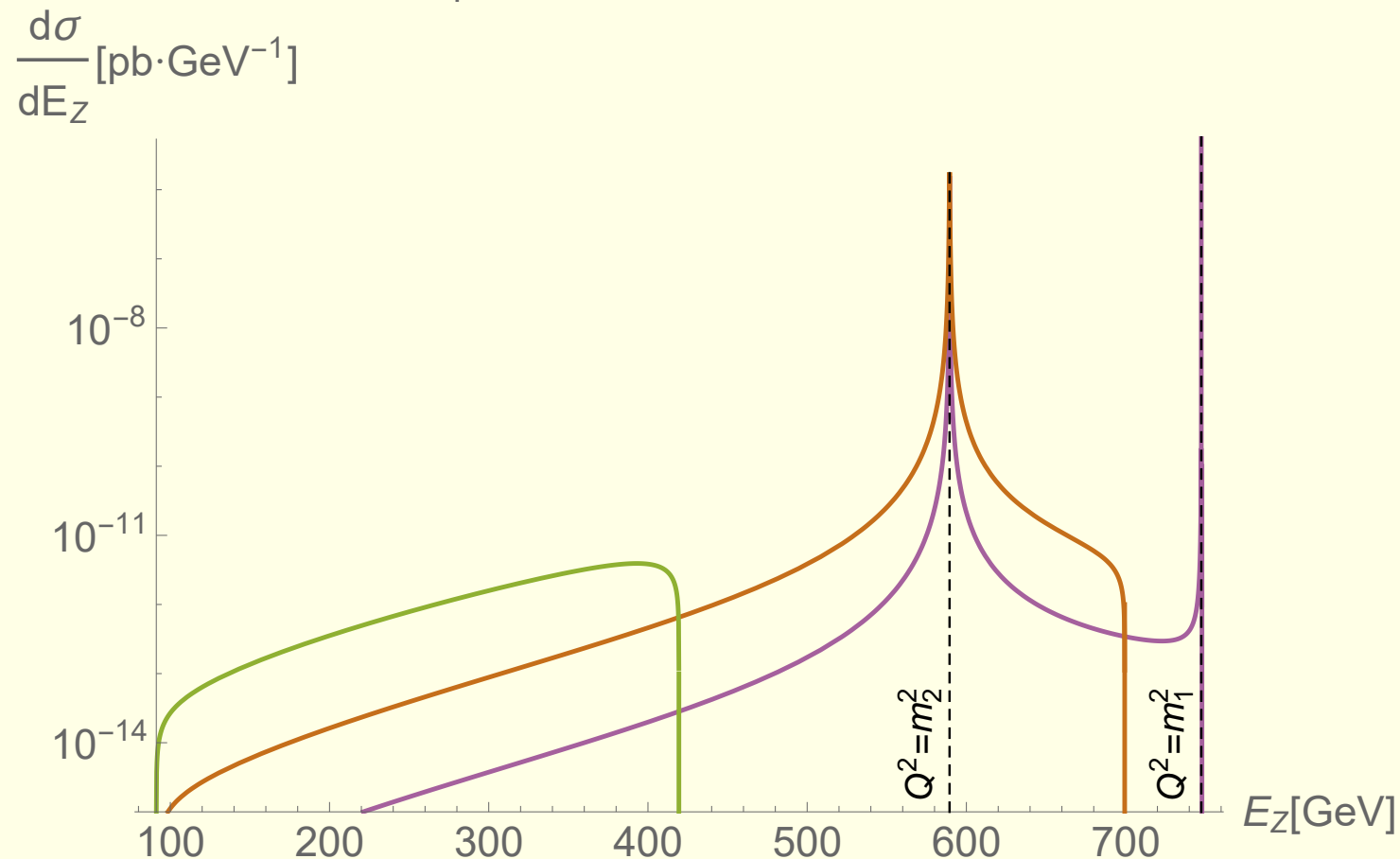
Figure 8: $\frac{d\sigma}{dE_Z}$ for the pGDM model.

$$E_Z(Q^2 = m_i^2) = E_i \equiv \frac{s - m_i^2 + m_Z^2}{2\sqrt{s}}, \quad E_{\text{max}} = \frac{s - 4m_{DM}^2 + m_Z^2}{2\sqrt{s}}$$

The strategy:

1. From the endpoint $E_{\max}$ one can determine $m_{DM}$:

$$E_{\max} = \frac{s - 4m_{DM}^2 + m_Z^2}{2\sqrt{s}},$$

2. In the presence of two poles, $m_2$ could be determined:

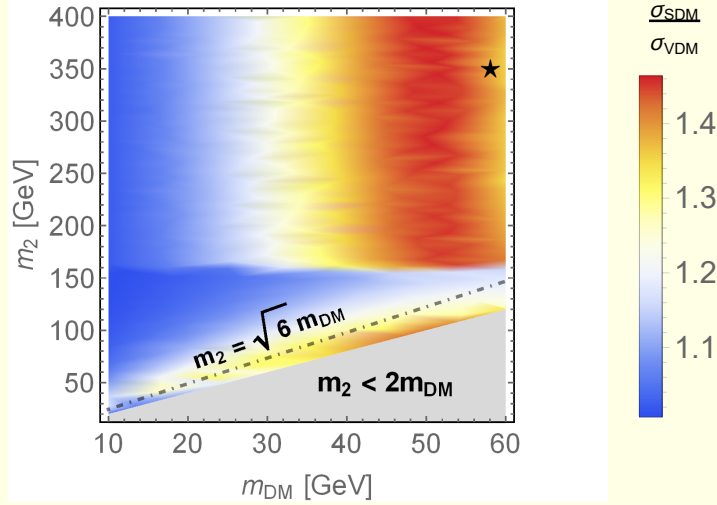$$E_Z(Q^2 = m_2^2) = E_2 \equiv \frac{s - m_2^2 + m_Z^2}{2\sqrt{s}}.$$

3. Then ratio

$$1 \lesssim \frac{\frac{d\sigma_{\text{pGDM}}}{dE_Z}}{\frac{d\sigma_{\text{VDM}}}{dE_Z}} \lesssim \frac{3}{2}$$
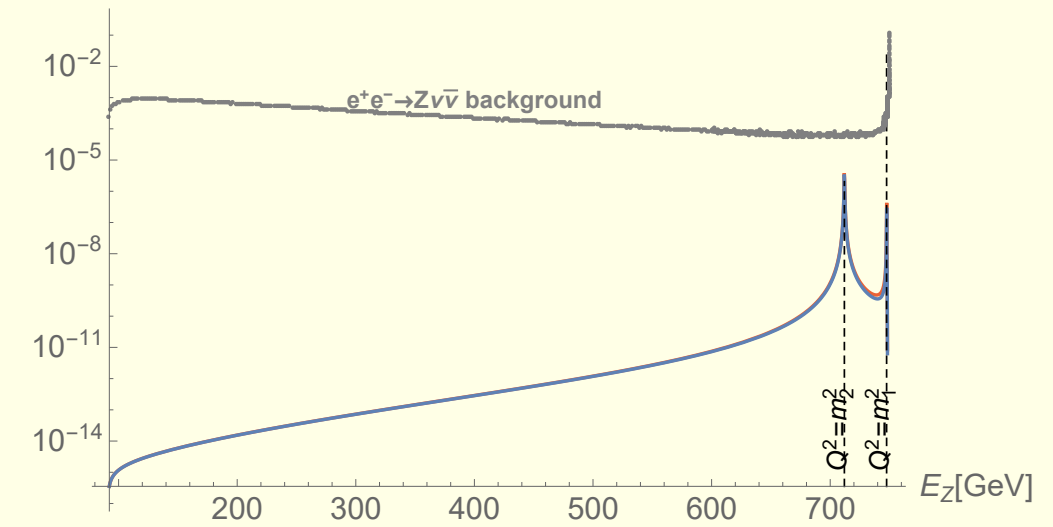
It is typically greater than 1.

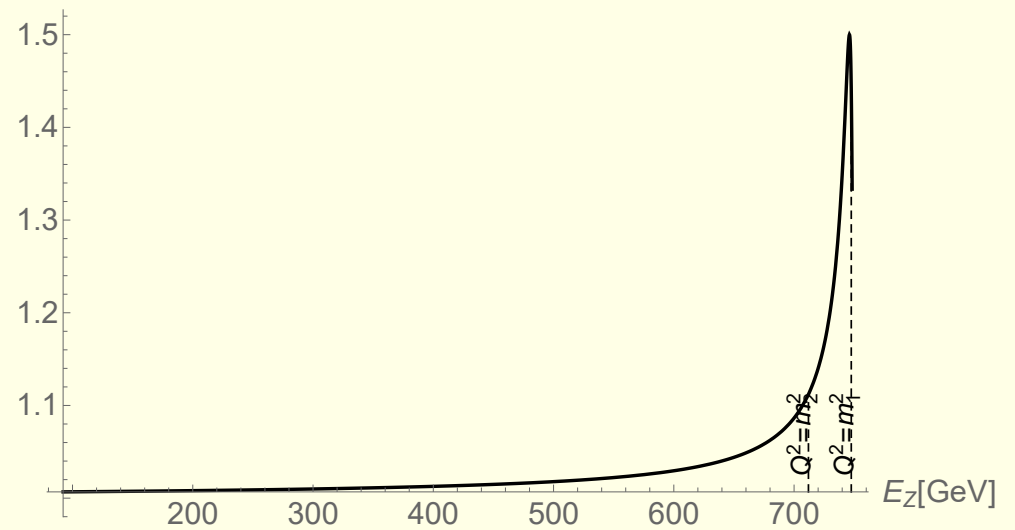4. If $m_i^2 \simeq 6m_{DM}^2$ the maximal deviation $(50\%)$ appears exactly at the $i$-th pole.

$\sqrt{s}$ = 1.5 TeV, $\sin\alpha$ = 0.29, $v_S$ = 5.54 TeV

$\dfrac{\sigma_{SDM}}{\sigma_{VDM}}$

$m_2 = \sqrt{6}\, m_{DM}$

$m_2 < 2m_{DM}$

$m_{DM}$ [GeV]

$m_2$ [GeV]

$\dfrac{d\sigma}{dE_Z}[\text{pb}\cdot\text{GeV}^{-1}]$

$e^+e^- \to Z\nu\bar{\nu}$ background

$Q^2 = m_2^2$

$Q^2 = m_1^2$

$E_Z$[GeV]

$\dfrac{d\sigma_{SDM}}{dE_Z} \Big/ \dfrac{d\sigma_{VDM}}{dE_Z}$

$Q^2 = m_2^2$

$Q^2 = m_1^2$

$E_Z$[GeV]

values in ★

$m_2 = 350$ GeV, $\quad m_{DM} = 58$ GeV

—— **scalar DM model**: $\sigma_{tot} = 3.1\times10^1$ ab

$\Gamma_1 = 3.6\times10^{-3}$ GeV, $\text{BR}_{h_1\to DM} = 0.6\,\%$

$\Gamma_2 = 1.8$ GeV, $\text{BR}_{h_2\to DM} = 0.7\,\%$

—— **vector DM model**: $\sigma_{tot} = 2.2\times10^1$ ab

$\Gamma_1 = 3.6\times10^{-3}$ GeV, $\text{BR}_{h_1\to DM} = 0.4\,\%$

$\Gamma_2 = 1.8$ GeV, $\text{BR}_{h_2\to DM} = 0.6\,\%$

$$\frac{d\sigma}{dE_Z} \propto \frac{\sqrt{1 - 4\frac{m_{DM}^2}{Q^2}}\cdot Q^4}{[(Q^2 - m_1^2)^2 + (m_1\Gamma_1)^2]\,[(Q^2 - m_2^2)^2 + (m_2\Gamma_1)^2]} \begin{cases} 1 & \text{(pGDM)} \\ 1 - 4\frac{m_X^2}{Q^2} + 12\left(\frac{m_X^2}{Q^2}\right)^2 & \text{(VDM)} \end{cases}$$
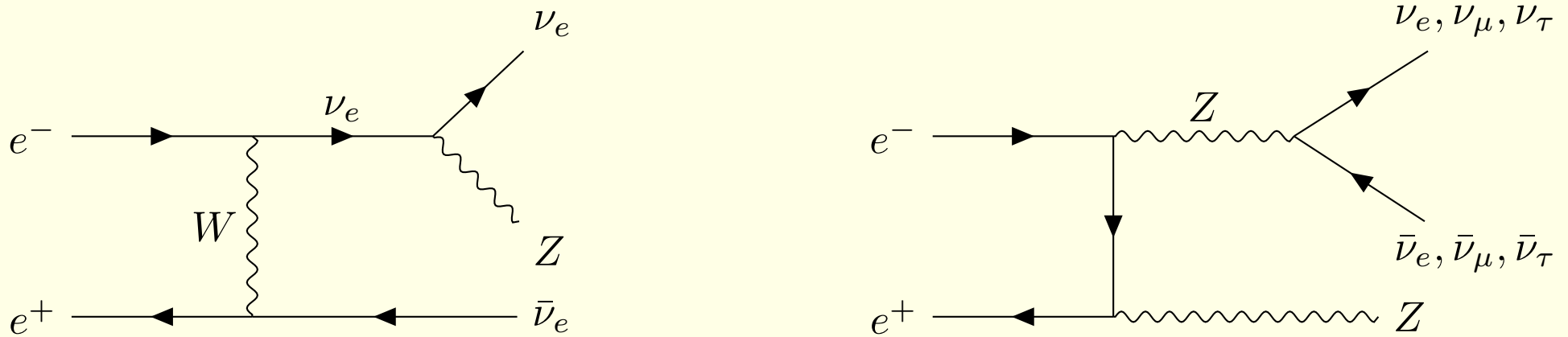
# Background



Figure 9: Exemplary diagrams of the Standard Model background processes. Neutrinos contribute to missing energy and can therefore mimic dark particles. The background cross-section could be reduced by polarizing the initial $e^+$ and $e^-$ beams.

# Comments

- Only a vicinity of a pole for one of the Higgs bosons, i.e. only events with $Z$ boson energy within a certain bin around $E_Z = E_i(\sqrt{s}) \equiv (s - m_i^2 + m_Z^2)/(2\sqrt{s})$ could be useful.

- For $\sqrt{s} = 1.5$ TeV, $m_{DM} = 44.5$ GeV, $m_2 = 102$ GeV, $v_S = 5$ TeV and $\sin\alpha = 0.31$ the separation between the cross-sections for pGDM and VDM at the level of $1\sigma$ could be obtained for a bin around $E_Z = E_1(1.5$ TeV$)$ with the width $\sim 4.5$ GeV.

- Jet energy can be measured in calorimeters with resolution $\sim 3\%$. Hence, the minimal size expected for the resolution of the $Z$ energy near the $h_1$ pole at,

  - CLIC with $\sqrt{s} = 1.5$ TeV is $\sim 3\% \times E_Z|_{E_Z=E_1(1.5\text{ TeV})} = 22.4$ GeV,
  - CEPC with $\sqrt{s} = 240$ GeV and the same parameters, for the minimal bin size $\sim 3\% \times E_Z|_{E_Z=E_1(240\text{ GeV})} = 3.1$ GeV the separation between the two cross-sections is at the level of $12\sigma$.

Therefore it is fair to conclude that there exist regions of parameters, where the two scenarios might be disentangled at future $e^+e^-$ colliders in resonance regions.

## Summary

1. The Abelian VDM model is challenged by an attractive pGDM model with DM candidate $A$ that is a pseudo-Goldstone boson related to $U(1)$ symmetry softly broken by $\mu^2(S^2 + S^{*\,2})$,

2. Vacuum stability in both models,

3. Direct detection efficiently suppressed in the pGDM model, $\sigma_{DM-N} \propto v_A^4$, as a consequence of $A$ being a pseudo-Goldstone boson, 1-loop calculations were performed and adopted, for $q^2 = 0$ the 1-loop results are UV finite and vanish in the limit $m_A = m_{DM} \to 0$,

4. In some regions of $(m_i, m_X)$ space $(m_i^2 \simeq 6m_X^2)$ $e^+e^-$ colliders might be useful to disentangle the models,

5. In some regions of the parameter space only pGDM could be realized.
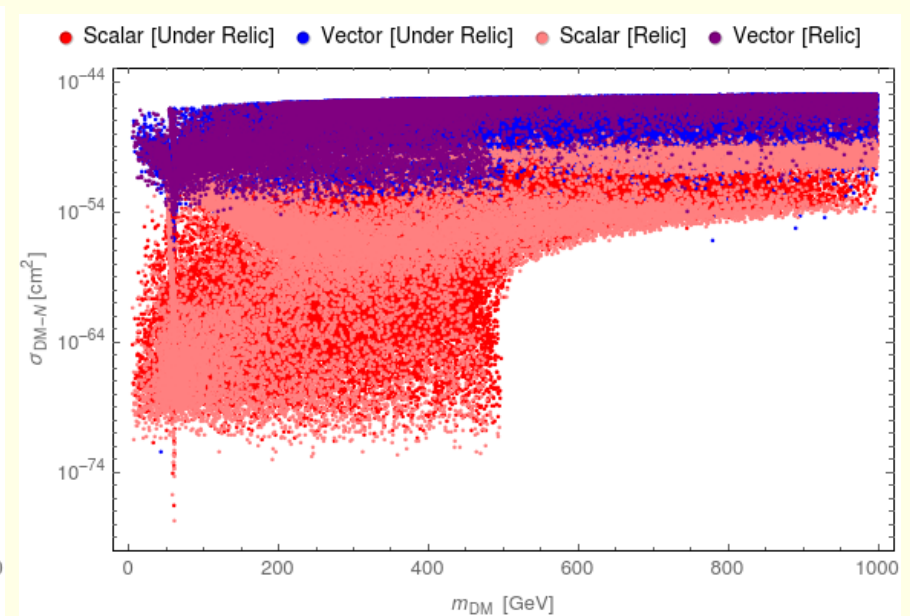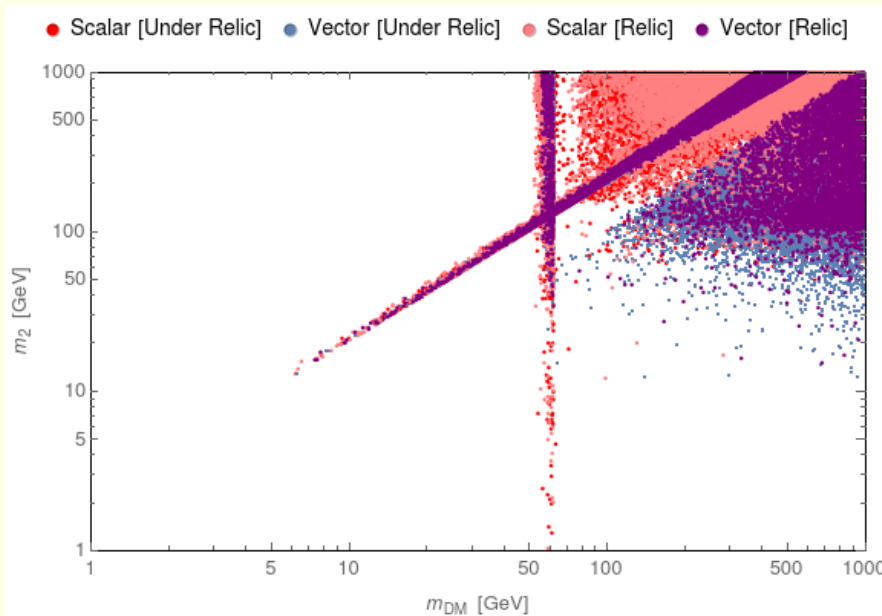
# Backup slides

## The global minimum for the pGDM:

$$v^2 = \frac{4\lambda_S\mu_H^2 - 2\kappa(\mu_S^2 - 2\mu^2)}{4\lambda_H\lambda_S - \kappa^2}, \quad v_S^2 = \frac{4\lambda_H(\mu_S^2 - 2\mu^2) - 2\kappa\mu_H^2}{4\lambda_H\lambda_S - \kappa^2}, \quad v_A^2 = 0$$

$$V_1 = \frac{-1}{4\lambda_H\lambda_S - \kappa^2} \left\{ \lambda_H(\mu_S^2 - 2\mu^2)^2 + \mu_H^2 \left[ \lambda_S\mu_H^2 - \kappa(\mu_S^2 - 2\mu^2) \right] \right\}$$

$$\mathcal{M}^2 = \begin{pmatrix} 2\lambda_H v^2 & \kappa v v_S & 0 \\ \kappa v v_S & 2\lambda_S v_S^2 & 0 \\ 0 & 0 & -4\mu^2 \end{pmatrix}$$

$$2\lambda_S\mu_H^2 > \kappa(\mu_S^2 - 2\mu^2) \ \text{ and } \ 2\lambda_H(\mu_S^2 - 2\mu^2) > \kappa\mu_H^2 \ \text{ and } \ \mu^2 < 0$$

$$\sigma_{AN}^{(1)} = \frac{f_N^2}{\pi v_H^2} \frac{m_N^2 \mu_{AN}^2}{m_A^2} \mathcal{F}^2,$$

where the one-loop function $\mathcal{F}$ is defined as

$$\mathcal{F} = \frac{V_{AA1}^{(1)} c_\alpha}{m_1^2} - \frac{V_{AA2}^{(1)} s_\alpha}{m_2^2}$$

with $V_{AA1,AA2}^{(1)}$ as one-loop corrections to the vertices $h_1 A^2$ and $h_2 A^2$.

$$\begin{aligned}
\mathcal{F} = & -\frac{s_{2\alpha}(m_1^2 - m_2^2)m_A^2}{128\pi^2 v_H v_S^3 m_1^2 m_2^2}[\mathcal{A}_1 C_2(0, m_A^2, m_A^2, m_1^2, m_2^2, m_A^2) \\
& + \mathcal{A}_2 D_3(0, 0, m_A^2, m_A^2, 0, m_A^2, m_1^2, m_1^2, m_2^2, m_A^2) \\
& + \mathcal{A}_3 D_3(0, 0, m_A^2, m_A^2, 0, m_A^2, m_1^2, m_2^2, m_2^2, m_A^2)]
\end{aligned}$$

$$\begin{aligned}
\mathcal{A}_1 & \equiv 4(m_1^2 s_\alpha^2 + m_2^2 c_\alpha^2)(2m_1^2 v_H s_\alpha^2 + 2m_2^2 v_H c_\alpha^2 - m_1^2 v_S s_{2\alpha} + m_2^2 v_S s_{2\alpha}), \\
\mathcal{A}_2 & \equiv -2m_1^4 s_\alpha[(m_1^2 + 5m_2^2)v_S c_\alpha - (m_1^2 - m_2^2)(v_S c_{3\alpha} + 4v_H s_\alpha^3)], \\
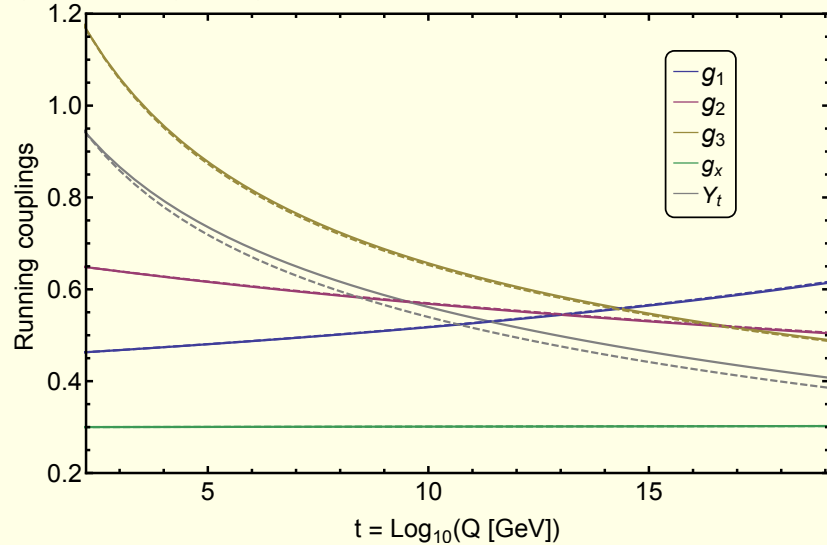\mathcal{A}_3 & \equiv 2m_2^4 c_\alpha[(5m_1^2 + m_2^2)v_S s_\alpha - (m_1^2 - m_2^2)(v_S s_{3\alpha} + 4v_H c_\alpha^3)].
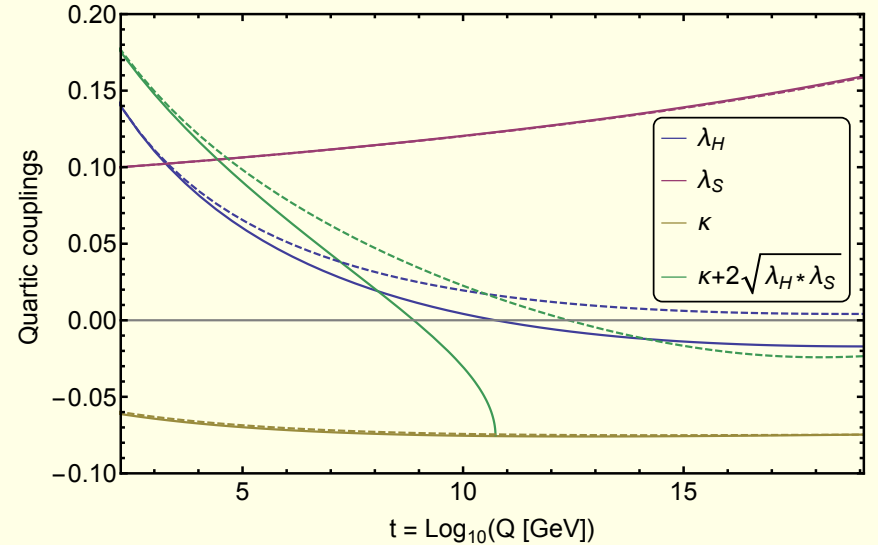\end{aligned}$$

Figure 10: Running of various parameters at 1- and 2-loop, in solid and dashed lines respectively. For this choice of parameters $\lambda_H(Q) > 0$ at 2-loop (right panel blue) but not at 1-loop. $\lambda_S(Q)$ is always positive (right panel red), running of $\kappa(Q)$ is very limited, however the third positivity condition $\kappa(Q) + 2\sqrt{\lambda_H(Q)\lambda_S(Q)} > 0$ is violated at higher scales even at 2-loops (right panel green).

The mass of the Higgs boson is known experimentally therefore within *the SM* the initial condition for running of $\lambda_H(Q)$ is fixed

$$\lambda_H(m_t) = M_{h_1}^2/(2v^2) = \lambda_{SM} = 0.13$$

For VDM this is not necessarily the case:

$$M_{h_1}^2 = \lambda_H v^2 + \lambda_S v_S^2 \pm \sqrt{\lambda_S^2 v_S^4 - 2\lambda_H \lambda_S v^2 v_S^2 + \lambda_H^2 v^4 + \kappa^2 v^2 v_S^4}.$$

VDM:

- Larger initial values of $\lambda_H$ such that $\lambda_H(m_t) > \lambda_{SM}$ are allowed delaying the instability (by shifting up the scale at which $\lambda_H(Q) < 0$).

- Even if the initial $\lambda_H$ is smaller than its SM value, $\lambda_H(m_t) < \lambda_{SM}$, still there is a chance to lift the instability scale if appropriate initial value of the portal coupling $\kappa(m_t)$ is chosen.
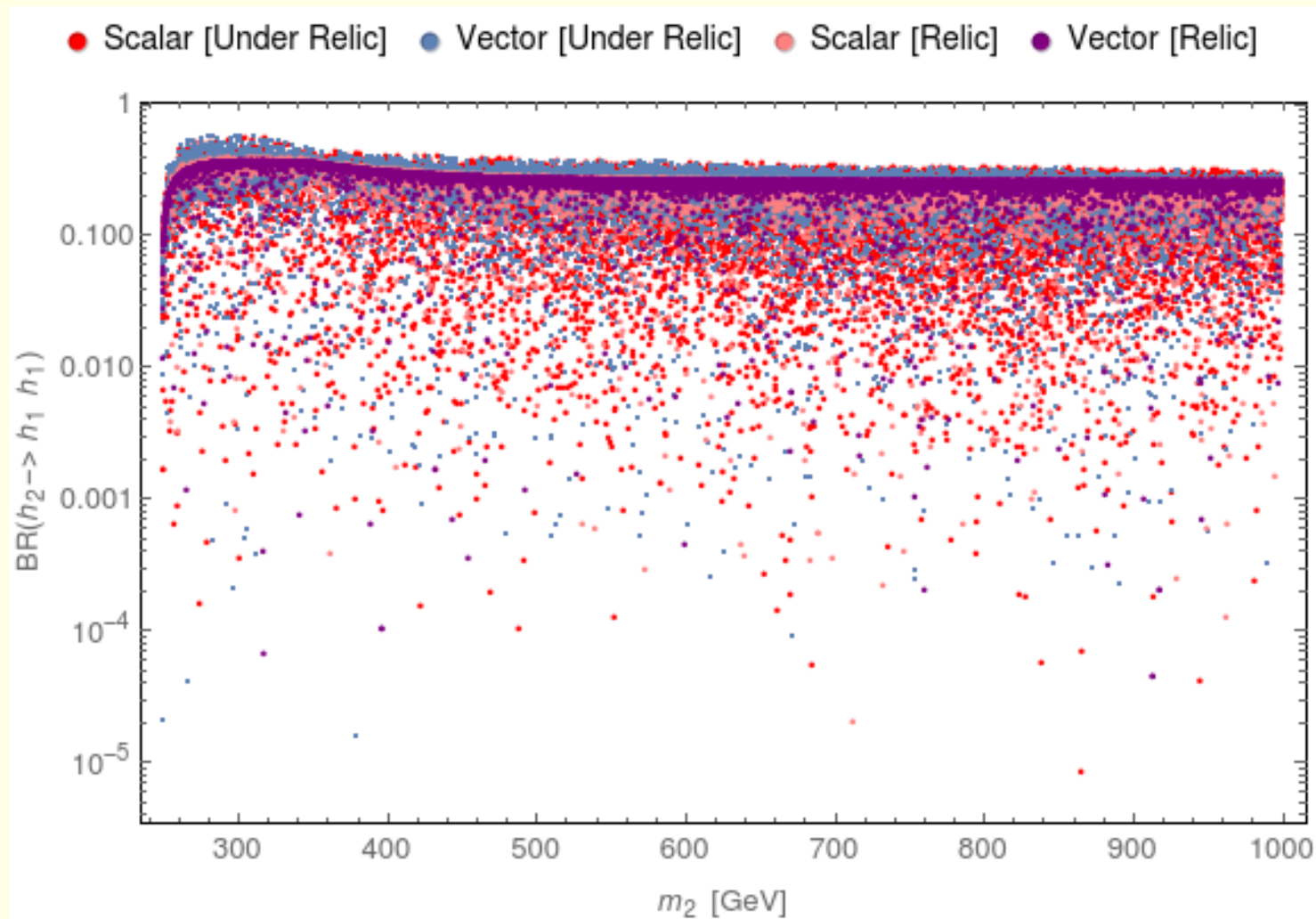$$\beta_{\lambda_H}^{(1)} = \beta_{\lambda_H}^{SM\ (1)} + \kappa^2$$

Figure 11: Branching ratio of second Higgs vs. mass of second Higgs. Scalar model in red, vector model in blue.
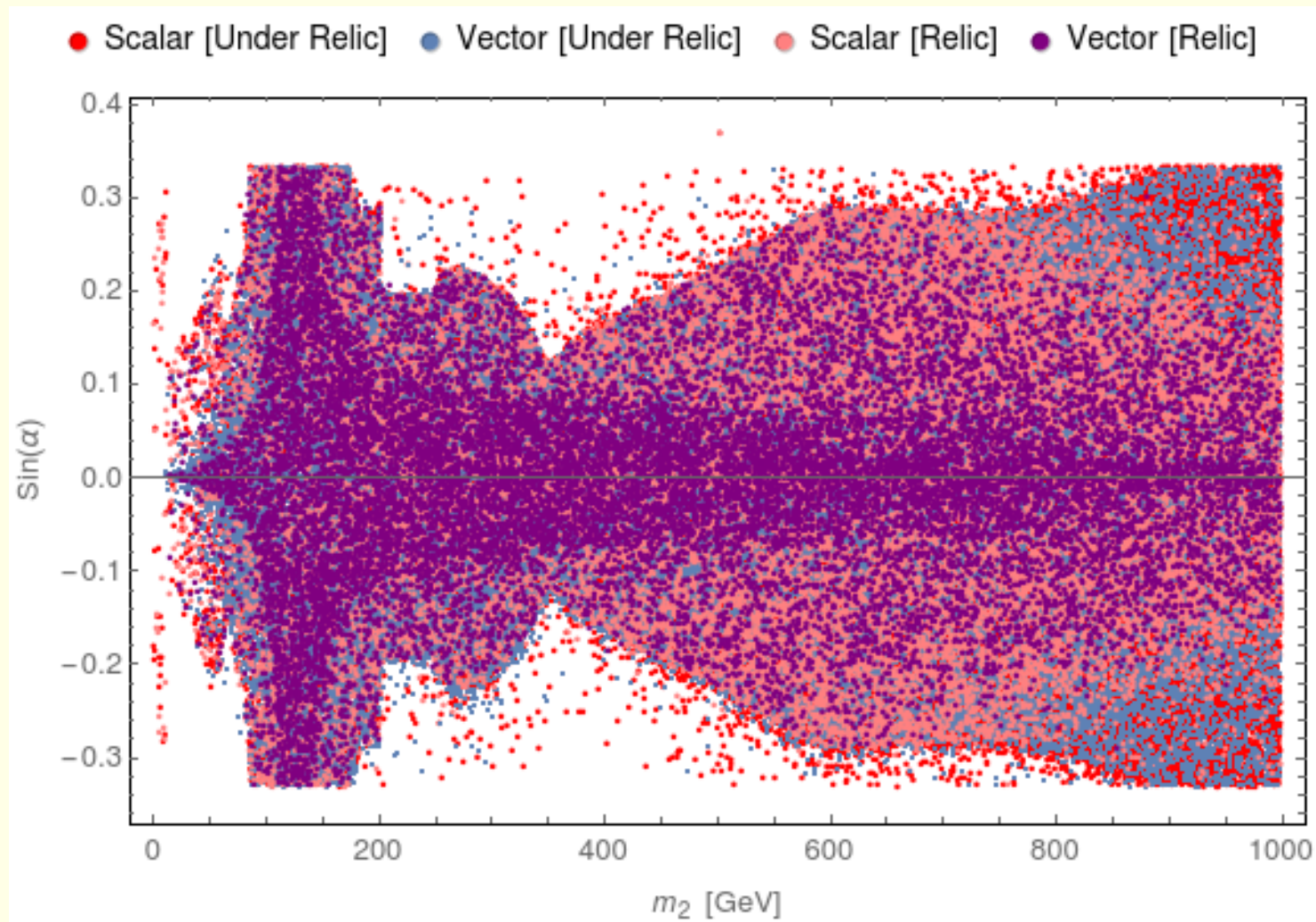
Figure 12: $\sin\alpha$ versus $m_2$.